

NASA/TM-2010-216838



Mode II Interlaminar Fracture Toughness and Fatigue Characterization of a Graphite Epoxy Composite Material

T. Kevin O'Brien
NASA Langley Research Center, Hampton, Virginia

William M. Johnston
Lockheed Martin, Hampton, Virginia

Gregory J. Toland
University of California, Santa Barbara, California

NASA STI Program . . . in Profile

Since its founding, NASA has been dedicated to the advancement of aeronautics and space science. The NASA scientific and technical information (STI) program plays a key part in helping NASA maintain this important role.

The NASA STI program operates under the auspices of the Agency Chief Information Officer. It collects, organizes, provides for archiving, and disseminates NASA's STI. The NASA STI program provides access to the NASA Aeronautics and Space Database and its public interface, the NASA Technical Report Server, thus providing one of the largest collections of aeronautical and space science STI in the world. Results are published in both non-NASA channels and by NASA in the NASA STI Report Series, which includes the following report types:

- **TECHNICAL PUBLICATION.** Reports of completed research or a major significant phase of research that present the results of NASA programs and include extensive data or theoretical analysis. Includes compilations of significant scientific and technical data and information deemed to be of continuing reference value. NASA counterpart of peer-reviewed formal professional papers, but having less stringent limitations on manuscript length and extent of graphic presentations.
- **TECHNICAL MEMORANDUM.** Scientific and technical findings that are preliminary or of specialized interest, e.g., quick release reports, working papers, and bibliographies that contain minimal annotation. Does not contain extensive analysis.
- **CONTRACTOR REPORT.** Scientific and technical findings by NASA-sponsored contractors and grantees.

- **CONFERENCE PUBLICATION.** Collected papers from scientific and technical conferences, symposia, seminars, or other meetings sponsored or co-sponsored by NASA.
- **SPECIAL PUBLICATION.** Scientific, technical, or historical information from NASA programs, projects, and missions, often concerned with subjects having substantial public interest.
- **TECHNICAL TRANSLATION.** English-language translations of foreign scientific and technical material pertinent to NASA's mission.

Specialized services also include creating custom thesauri, building customized databases, and organizing and publishing research results.

For more information about the NASA STI program, see the following:

- Access the NASA STI program home page at <http://www.sti.nasa.gov>
- E-mail your question via the Internet to help@sti.nasa.gov
- Fax your question to the NASA STI Help Desk at 443-757-5803
- Phone the NASA STI Help Desk at 443-757-5802
- Write to:
NASA STI Help Desk
NASA Center for AeroSpace Information
7115 Standard Drive
Hanover, MD 21076-1320

NASA/TM-2010-216838



Mode II Interlaminar Fracture Toughness and Fatigue Characterization of a Graphite Epoxy Composite Material

T. Kevin O'Brien
NASA Langley Research Center, Hampton, Virginia

William M. Johnston
Lockheed Martin, Hampton, Virginia

Gregory J. Toland
University of California, Santa Barbara, California

National Aeronautics and
Space Administration

Langley Research Center
Hampton, Virginia 23681-2199

August 2010

Trade names and trademarks are used in this report for identification only. Their usage does not constitute an official endorsement, either expressed or implied, by the National Aeronautics and Space Administration.

Available from:

NASA Center for AeroSpace Information
7115 Standard Drive
Hanover, MD 21076-1320
443-757-5802

Abstract

Mode II interlaminar fracture toughness and delamination onset and growth characterization data were generated for IM7/8552 graphite epoxy composite materials from two suppliers for use in fracture mechanics analyses. Both the fracture toughness testing and the fatigue testing were conducted using the End-notched Flexure (ENF) test. The ENF test for mode II fracture toughness is currently under review by ASTM as a potential standard test method. This current draft ASTM protocol was used as a guide to conduct the tests on the IM7/8552 material. The results for material produced by the two suppliers were similar for all material property values measured. The insight gained is valuable for current and future material property standards development. The draft ASTM procedure for G_{IIc} was followed, and produced consistently repeatable interlaminar fracture toughness values. Furthermore, the testing procedures developed in this study, and the associated test results, will be useful for developing mode II fatigue standards. Methods were developed to parse and analyze fatigue data. Development of a Mode II fatigue delamination onset curve for precracked specimens and specimens with inserts was discussed. The effects of performing material property tests from either precracks or inserts were discussed and compared. Testing from a precracked specimen gave more conservative properties than testing from an insert, for both interlaminar fracture toughness and fatigue onset data.

Introduction

As part of the Space Act Agreement (SAA) between the Center for Rotorcraft Innovation (CRI) and NASA Langley Research Center, fracture mechanics based analyses are being performed to predict delamination onset and growth in structural subcomponents made of IM7/8552 carbon-epoxy composite materials*. Delamination characterization data for opening (mode I) and shear (mode II) fracture modes are needed as input to these models. The mode II characterization of this material includes the testing of fracture toughness during static loading and the determination of delamination onset and growth during fatigue loading. Both the fracture toughness testing and the fatigue testing were conducted using the End-notched Flexure (ENF) test. The ENF test for mode II fracture toughness is currently under review by ASTM as a potential standard test method [1]. This current draft ASTM protocol was used as a guide to conduct the tests on the IM7/8552 material. There is no current ASTM standard for conducting Mode II fatigue delamination characterization. This report summarizes the test approach, methods, procedures and results of this characterization effort.

Experimental Scope and Approach

Characterization tests were conducted on IM7/8552 ENF coupons produced by two different rotorcraft manufacturers and made to their own specifications. The Mode II characterization included both the determination of the interlaminar fracture toughness, G_{IIC} , as well as the fatigue delamination onset and growth.

Tests were conducted using the End-notched Flexure specimen. The ENF test involves loading a beam with a mid-plane starter crack at one end, in three-point bending, as shown in figure 1. Crack length, a , is measured from the support roller, and the half-

* The terms “delamination” and “crack” will be used interchangeably throughout this report.

span length, L , is the distance from the support rollers to the center loading roller. A compliance calibration (CC) was performed for each specimen, before testing, to determine the relationship between specimen compliance and crack length. The compliance calibration relationship was used to estimate the crack length and to determine strain energy release rate (G) levels during the fracture and fatigue tests. Fracture tests were conducted according to the ASTM Draft Standard. Non-precracked (NPC) and precracked (PC) fracture toughnesses were determined for each specimen. A thin polytetrafluoroethylene (PTFE, or Teflon[®]) film was inserted on the mid-plane to act as a crack starter for the NPC tests. The specimens were pre-cracked from this Teflon insert during the NPC fracture test to create a naturally occurring crack, from which to propagate the crack in the subsequent PC tests. Fracture testing was conducted on a total of 5 specimens from each manufacturer to determine G_{IIC} . The average mode II fracture-toughness was calculated for each material group.

Fatigue characterization tests were run in load control at four different maximum cyclic loads, corresponding to initial $G_{II\max}$ values of 50%, 40%, 30%, and 20% of the average value of the PC G_{IIC} from the fracture toughness tests for each material manufacturer. Five specimens were tested at each applied load level. Specimens were precracked using the same procedure as the static specimens. The compliance calibration method was used to determine the crack length and G levels during the test. After testing, specimens were pulled apart and the initial and final crack length and crack front shapes were measured. These revised crack lengths were used in the final data reduction. Crack growth rate was determined as a function of the maximum applied energy release rate, $G_{II\max}$. The number of cycles before fatigue delamination growth onset occurred was also determined.

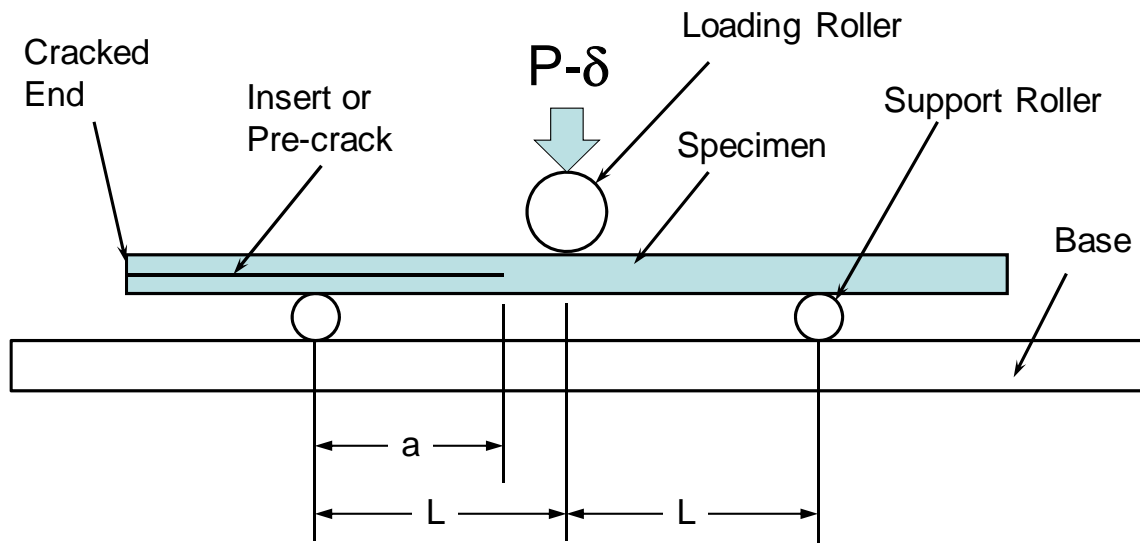


Fig.1. End-notched Flexure (ENF) 3-point bend test

Test set up and procedure

Twenty-four ply, zero-degree unidirectional test coupons, measuring 7.0 inches long by 1.0 inch wide, were manufactured for this study by each of the two manufacturers. Specimens were nominally 0.175 inches thick. Actual specimen thicknesses and widths, measured at three locations along the length and averaged, are shown in Appendix 1 for both manufacturers (referred to as Source 1 and Source 2). A 3.0-inch long, 0.0005-inch thick, polytetrafluoroethylene (PTFE or Teflon®) film was embedded in one end at the mid-plane of the specimen thickness, across the 1.0-inch width of the test specimen, to act as a crack starter. The specimen edges were coated with a white spray paint to easily view the onset of delamination from the insert

Non-precracked Fracture Toughness Tests from the Teflon Insert

All specimens, including those tested in fatigue, were first statically precracked from the insert (NPC testing). Figure 2a shows a schematic of the specimen and non-precracked testing dimensions that were used for the NPC fracture test. Figure 2b shows a test specimen in the three-point bend fixture. This configuration was used to generate the NPC fracture toughness and a shear pre-crack of approximately 0.5 inches from the end of the insert. The end of the PTFE film was located at 3.0 inches from the cracked end and placed 1.5 inches from the left roller for fracture testing. Tick marks were made on the specimen at 3.5 inches from the cracked end, and at +0.4 and -0.4 inches away from this mark, to use as guides for positioning the center load nose during compliance calibration loadings. The compliance calibration and NPC fracture test consisted of three loadings. The first two loadings used a maximum load below the failure load, so as not to cause delamination growth. First, the specimen was positioned in the three-point-bend fixture with the center load nose above the +0.4 mark and loaded to produce a plot of load versus stroke to obtain the specimen compliance. Next, the specimen was shifted to align the center load nose with the -0.4 inch mark, and the specimen was reloaded to determine the compliance again. Finally, the specimen was repositioned in the three-point-bend fixture to the testing position (center tick mark under the center load nose) as shown in figure 2, loaded until the crack extended, and then unloaded. Load and displacement were recorded through the complete load-unload cycle. The initial loading data prior to crack growth provided a third compliance value for the compliance calibration. The unloading compliance after fracture occurred was used with the compliance calibration to calculate the precrack length. During the NPC fracture test, the delamination grew about 0.5 inches from the end of the insert to the vicinity of the central load nose. Photos taken after unloading (figure 3) showed the two specimen edges and provided a visual reference of the crack length (insert length from first roller plus pre-crack). The tick marks used for aligning the specimens for the CC loadings are also shown in the photo. The crack length, a , after NPC testing was approximately 2.0 inches.

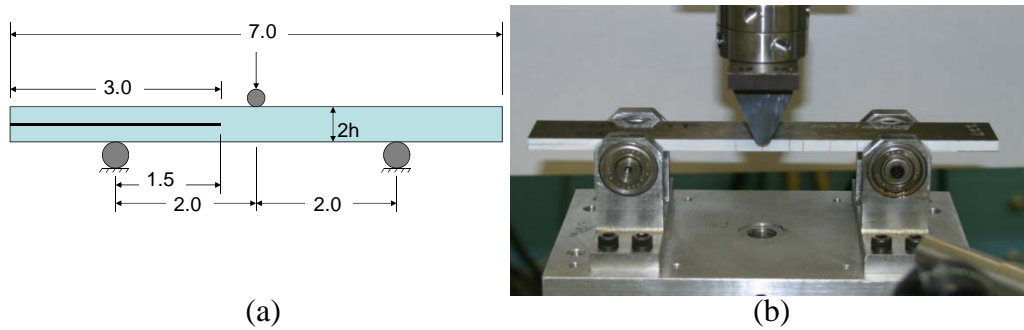


Fig.2 Static ENF pre-cracking test configuration (dimensions are in inches)

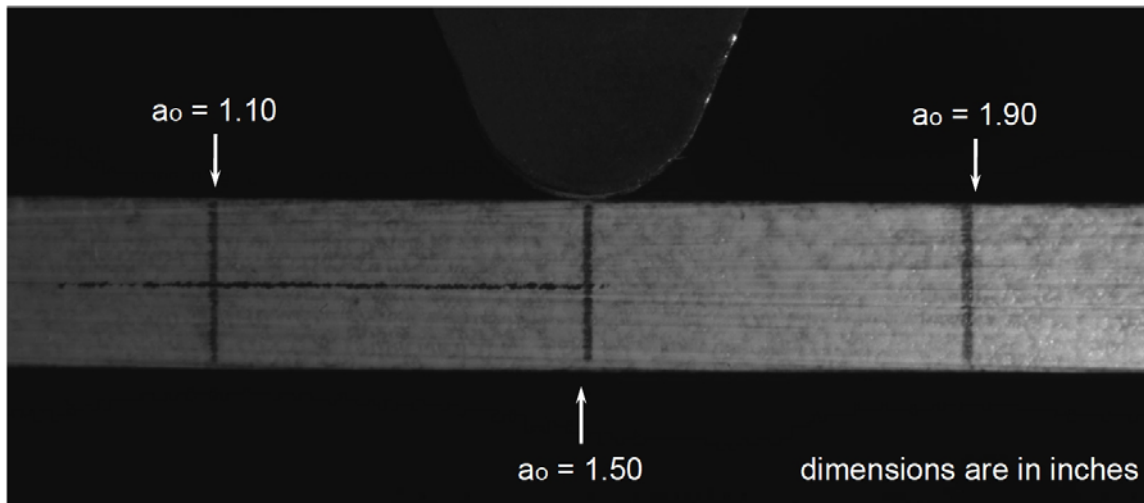


Fig.3 Specimen edge showing crack growth past the central loading nose.

Precracked Fracture Toughness Tests

After precracking the specimen during the NPC fracture test, the specimen was ready for PC fracture testing. The specimen is shown in the PC fracture testing configuration in the three-point-bend fixture in figure 4a. The location of the center load nose was marked on the specimen at approximately 4.5 inches from the cracked end. The end of the shear pre-crack was placed 1.0 inch from the left roller. Figure 4b shows the specimen prior to testing in the three-point bend fixture. A compliance calibration was completed with the pre-cracked specimen prior to testing. Tick marks were made on the specimen edges at +0.4 and -0.4 inches from the center load nose mark for positioning the specimen for the precracked compliance calibration loadings. The specimen was shifted so that the center load nose was positioned first above the +0.4 mark, and then above the -0.4 inch mark, and loaded in each case to yield a plot of load versus stroke to obtain the specimen compliance, keeping the load below a level that would cause further delamination growth. In order to measure a pre-cracked value of G_{IIC} , the specimen was shifted to the testing position as shown in figure 4, and the specimen was loaded until the crack extended, and then unloaded. The initial loading portion of the test was used for the third compliance calibration run. The delamination grew about 1.0 inch, from the initial 1.0-inch crack length at the end of the shear precrack to near the central load nose.

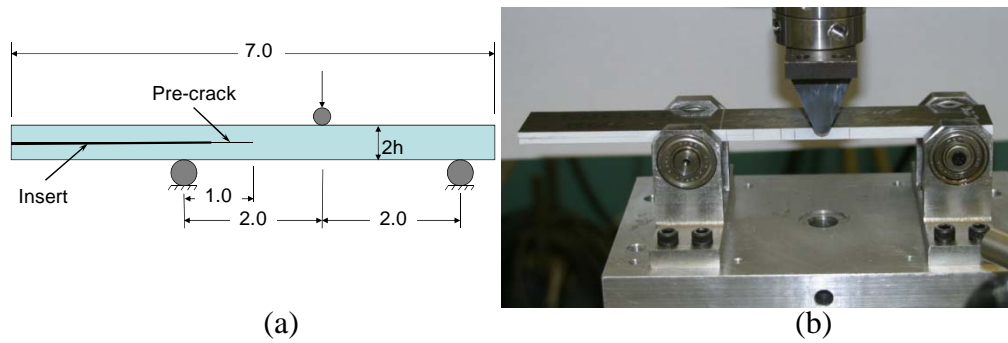


Fig.4 ENF test configuration with a pre-cracked specimen (dimensions are in inches)

Fatigue Testing

To conduct fatigue tests to measure delamination onset and growth, precracked specimens were placed in the fixture as shown in figure 4. The specimens were then subjected to a sinusoidal cyclic loading at a frequency of 5 Hz, and a stress ratio (P_{min}/P_{max}) of $R = 0.1$. Tests were conducted in load control using the Fracture Technology Associates (FTA) software for data accumulation and retrieval [2]. Tests were run at maximum cyclic loads, P_{max} , corresponding to $G_{II_{max}}$ values equal to 50%, 40%, 30%, and 20% of the average value of G_{IIC} from the pre-cracked fracture tests. Prior to fatigue testing, a compliance calibration was conducted to determine the relationship between compliance and crack length and to calculate the appropriate P_{max} , for each of five specimens being tested at the same $G_{II_{max}}$ value. For all three crack lengths used to obtain this compliance calibration, the load was kept below a level that would cause further delamination growth. During fatigue, the compliance was measured at a constant interval of cycles until the test was stopped. This interval was either every 2 or 10 cycles. The FTA system monitored compliance and calculated a corresponding crack length. The system stopped cycling when the calculated crack length reached 2 inches. During fatigue the delamination grew about 1.0 inch from the shear precrack to the vicinity of the central load nose. After unloading, the specimens were pried open to allow measurement of the initial and final crack front shapes. Photos were taken of the two specimen surfaces to obtain a visual reference of the crack lengths and shapes.

Data reduction

Data reduction was conducted to produce fracture toughness and fatigue properties. Compliance calibration was used before and after precracking for all of the specimens to determine G levels. The compliance calibration was also used in the fatigue tests to determine crack length. Fracture toughness was calculated from both the PC and NPC tests. Fatigue data was reduced to produce delamination onset and growth curves.

Compliance Calibration

The CC method was first performed on the NPC fracture tests as follows. Three loadings were used to obtain three plots of compliances versus crack length. The three compliances are those from the two CC tests (at $a_o-0.4 = 1.1$ inches, and $a_o+0.4 = 1.9$ inches) and from the initial portion of the fracture test ($a_o = 1.5$ inches). Figure 5 shows typical compliance calibration load-displacement plots from the NPC fracture test. Figure 6 shows a typical ENF load-displacement plot from the NPC fracture test.

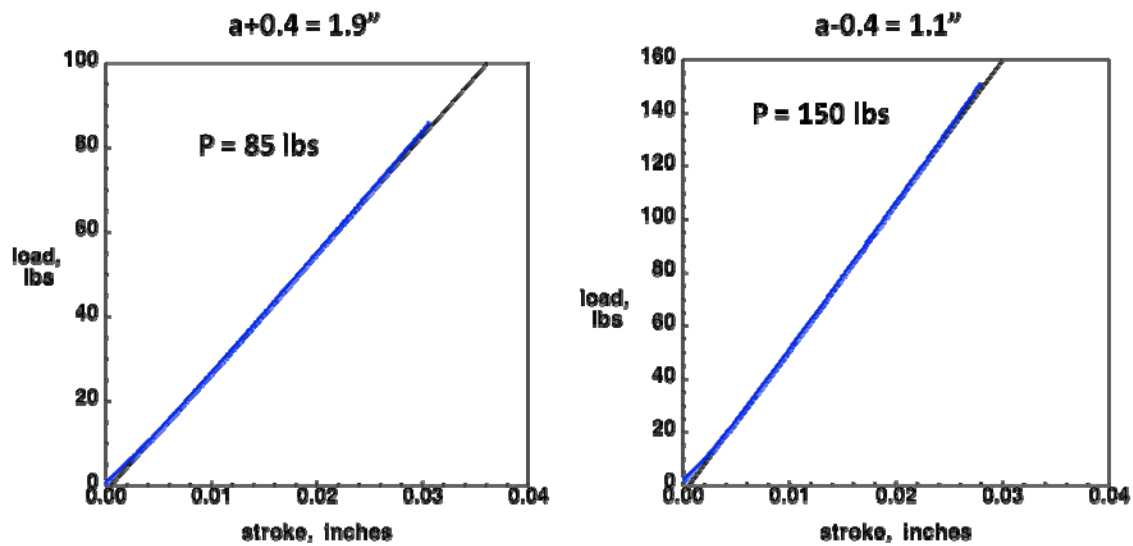


Fig. 5 Typical Compliance Calibration load displacement plots

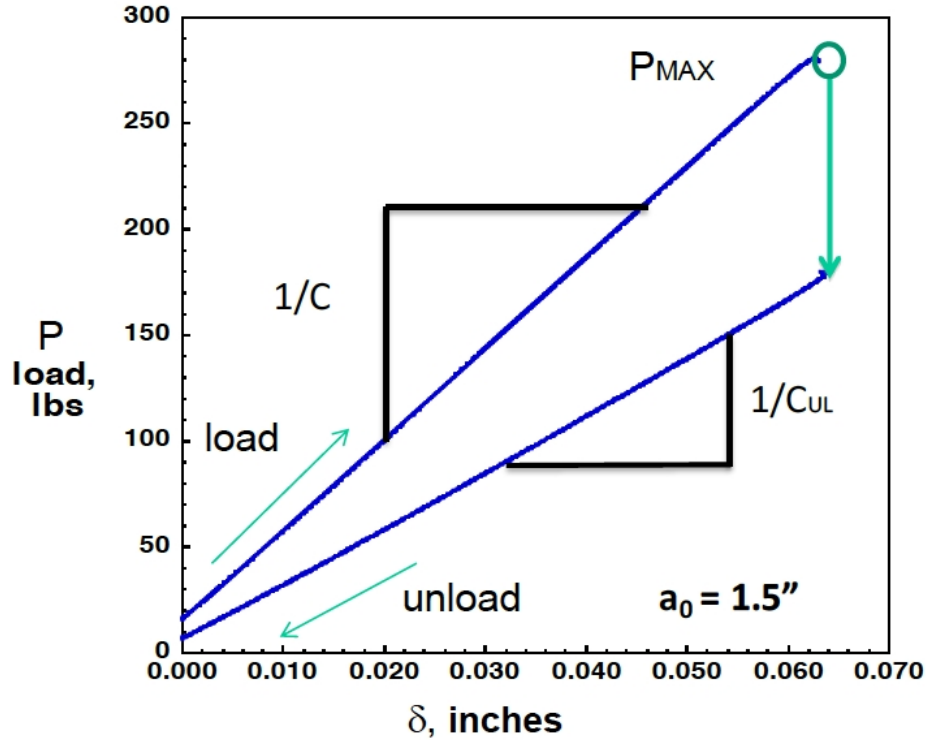


Fig. 6 Typical fracture test load-displacement plot

At each crack length, the compliance was determined by a least-squares linear regression analysis of the digital data to obtain the slope of the displacement versus load (δ vs P) data. The resulting compliances were plotted against the corresponding crack lengths raised to the third power and fit a line given by equation 1.

$$C = A + ma^3 \quad (1)$$

The CC coefficients, m and A , were determined using a least-squares linear regression analysis of the compliance, C , versus crack length cubed (a^3) where A is the intercept and m is the slope obtained from the regression analysis. Rearranging equation 1, yields a relationship between crack length and compliance, as shown in Equation 2.

$$a = \left(\frac{C - A}{m} \right)^{1/3} \quad (2)$$

Figure 7 shows a typical NPC fracture test fit of compliance as a function of crack length. During the NPC fracture test from the PTFE insert, the crack did not always grow to a length of exactly 2.0 inches under the load nose. Therefore, the unloading modulus, C_{UL} , was measured to estimate the actual crack length from equation 2.

This calculated crack length was used to determine the initial conditions for the PC fracture tests and the fatigue tests. For each specimen, the difference between this estimated crack length and the nominal final crack length of 2.0 inches was added to the assumed 1.0 inch initial crack length for the pre-crack configuration, shown in figure 4, to perform the compliance calibration on the precracked specimens. The pre-cracked compliance calibration was performed using the same procedure as for the NPC specimens, starting from the configuration shown in figure 4. The new values of A and m from equation 1 from this pre-cracked compliance calibration were then used to determine the PC G_{IIc} , and to estimate the maximum cyclic load levels for the fatigue tests. All of the compliance calibration coefficients from the NPC and PC tests are presented in Appendix 1.

The energy release rate, G_{II} , was determined using the compliance calibration relation specified in the ASTM draft standard [1]. Equation 3 shows the equation for G_{II} for a specimen with a constant width, B . Substituting the compliance relation from Equation 1 into Equation 3 and taking the derivative, yields equation 4, where G_{II} is a function of the compliance calibration constant, m .

$$G_{II} = \frac{P^2}{2B} \frac{\partial C}{\partial a} \quad (3)$$

$$G_{II} = \frac{3mP^2 a^2}{2B} \quad (4)$$

The compliance calibration data and equation 4 were used to calculate G_{IIc} and maximum cyclic G_{II} levels.

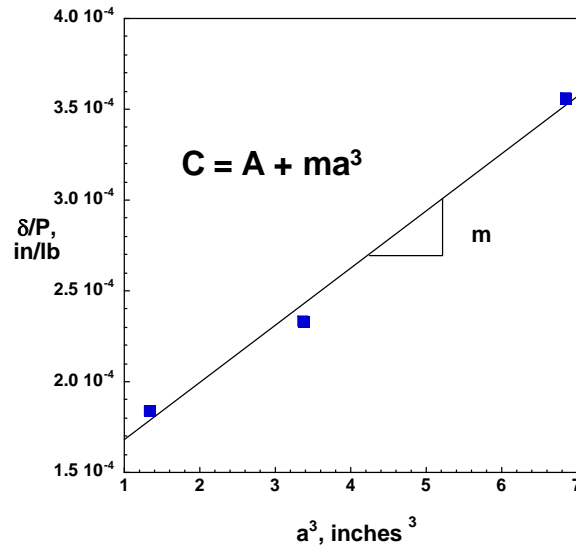


Fig.7 Typical fit of compliance as a function of crack length for NPC fracture test.

Fracture Toughness Calculations

The mode II NPC and PC fracture toughness was determined using equation 4, where m is the CC coefficient, P is the maximum load from the fracture test, a is the initial crack length, and B is the specimen width. As a further check on the estimated crack lengths, test specimens were pried open following final failure. Using the end of the PTFE film and the tick marks as guides, the initial delamination lengths were corrected, providing accurately measured values.

Fatigue Property Calculations

Fatigue tests were conducted at maximum cyclic G_{II} levels corresponding to 50%, 40%, 30%, and 20% of the average pre-cracked G_{IIc} for each source. These maximum cyclic load levels were obtained by solving equation 4 for P (equation 5) and then substituting the appropriate $G_{II\max}$ value.

$$P_{\max} = \frac{1}{a_0} \left(\frac{2BG_{II\max}}{3m} \right)^{1/2} \quad (5)$$

As a method to validate and correct the compliance calibration estimated crack lengths, all test specimens were pried open following fatigue loading. Figure 8 shows the fracture surface of a typical ENF fatigue specimen. It was possible to clearly delineate the end of the PTFE film, the end of the static pre-crack, the cyclic growth region, and the final crack length where the specimen was pried open. The precrack does not always coincide exactly with the tick marks on the edges of the specimen where the loading nose was aligned. Therefore, the initial pre-crack length was corrected based on these measurements, and the corrected value was used to perform the compliance calibration before finally reducing the data.

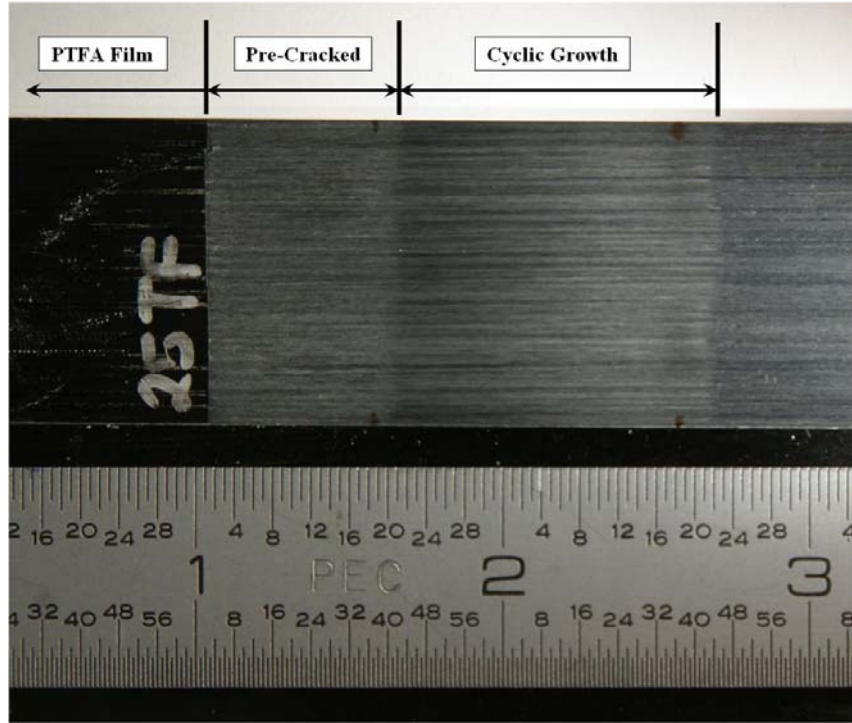


Fig.8 Fracture surfaces of typical ENF fatigue specimen

The FTA data acquisition system used during the fatigue tests provided compliance as a function of cycle count. To determine crack growth rate as a function of $G_{II\max}$, the compliance data were initially converted to crack length using Equation 2 and the CC data for the specimens (Figure 9). The derivative was taken numerically to provide the crack growth rate, da/dN .

Because the data sets produced were large and contained noise, compliance was recorded at 2-cycle intervals for the 50% G_{IIc} tests and at 10-cycle intervals for the 20-40% G_{IIc} tests to ensure that no data were lost. These intervals were not optimized to ensure a significant (above the noise level) increment of crack growth. To remedy this, the data were parsed to remove any crack growth interval of less than 0.002 inches, which was about twice the noise level in the data. The raw data and the resultant parsed data for one specimen are shown in Figure 10a. These parsed data were then analyzed to determine the crack growth rate.

The fatigue crack growth rate, da/dN , was calculated from the parsed data using the secant method and the incremental polynomial method, described in ASTM E647 [4]. Using the secant method, fatigue crack growth rate was calculated as,

$$da/dN = \frac{a_{i+1} - a_i}{N_{i+1} - N_i} \quad (6)$$

where a_i is a crack length corresponding to cycle count N_i , and a_{i+1} and N_{i+1} are crack length and cycle count values corresponding to the next available data point. The crack

length used to calculate G from this two point linear fit method is taken as the midpoint (average a) of the crack growth increment. Using the incremental polynomial method helps reduce error induced by noisy experimental data. The incremental polynomial method fits a parabola to successive sets of seven points of data. The fatigue growth rate is calculated as the derivative of this fit evaluated at the center point. The crack length used to calculate G is also taken from the center of the fit. The maximum cyclic G level was determined by substituting the estimated crack length and cyclic load for each growth rate measurement into equation 4. The data were plotted in the typical log-log form used for Paris law crack growth [5]. Typical results for fatigue crack growth are shown for the secant (2-point) and the sliding polynomial (7-point) data. The difference between the two reduction methods is illustrated in figure 10b. The sliding polynomial had significantly lower noise in the reduced data. For this paper the sliding polynomial method was used to reduce all of the crack growth vs. $G_{II\max}$ data.

The section of the curve that represented stable fatigue crack growth was isolated and analyzed. The lower limit of this curve was taken as the delamination onset point. The upper end of the linear region was determined visually and extracted to synthesize the delamination growth law. For each test specimen, the linear region data were plotted in the typical log-log form of a Paris law and the data were fit to a relationship in the form of Equation 7.

$$\frac{da}{dN} = DG_{II\max}^n \quad (7)$$

The data beyond the linear growth region of the curve were truncated. The data from each source were combined and fit to a single growth law equation. The data were also fit separately for each of the five load levels for each manufacturer.

The reduced crack growth rate data are shown in Figure 11 for an entire fatigue test. The onset and growth regions are determined from these data. The onset of delamination growth was defined as the point where da/dN reaches its absolute minimum. The crack length corresponding to the minimum da/dN value was then used to linearly interpolate the corresponding compliance and cycle count from the parsed data. The cycle count was recorded and used to formulate $G_{II\max}$ vs. N onset curves and the associated change in compliance was also recorded. This curve represents the threshold when stable fatigue crack growth begins. Onset curves were developed for each manufacturer and a combined curve for the material was also generated using all of the data.

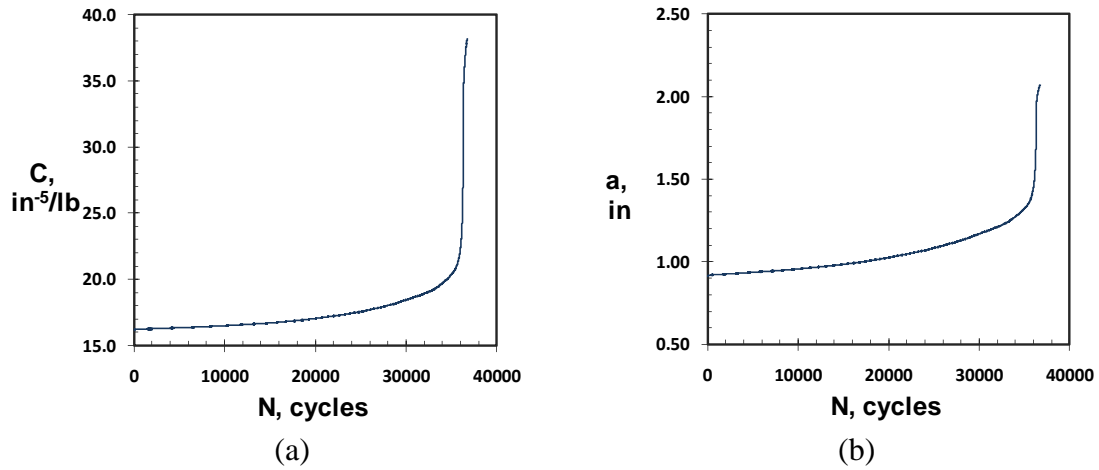


Fig.9 Typical plot of compliance (a) and crack length (b) as a function of fatigue cycles.

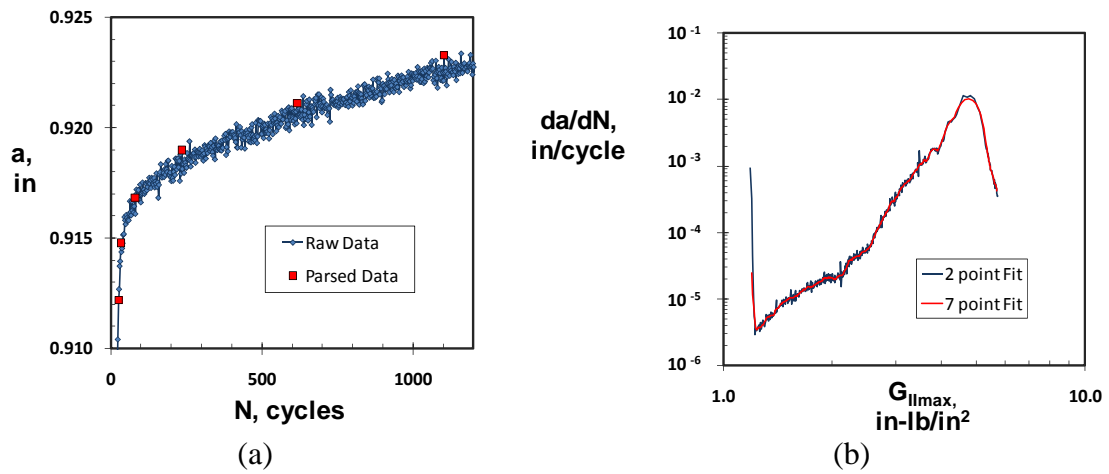


Fig.10 Typical plot of (a) raw and parsed crack length data as a function of fatigue cycles and (b) reduced crack growth data using both ASTM E647 data reduction methods.

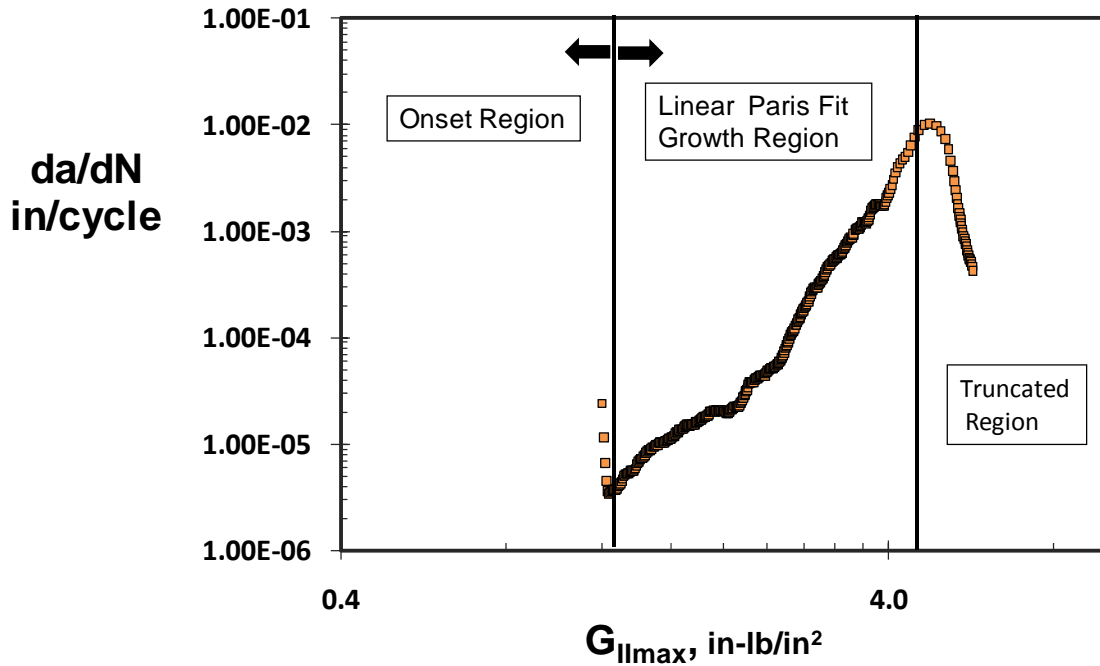


Fig.11 Reduced fatigue crack growth data with the onset and growth regions shown.

Fracture and Fatigue Test Results

Fracture toughness results for the NPC and PC fracture tests are shown in figure 12 for both sources of the material. The individual data points appear alongside an average value with corresponding error bars. The fracture test from the Teflon inserts (NPC tests) had significantly higher toughness than the shear precracked specimens (PC tests). The coefficient of variation for the precracked data is less than 10% and the data is reasonably consistent between the two manufacturers. The non pre-crack and the pre-crack mode II interlaminar fracture toughness data measurements for both sources are given in table 2.

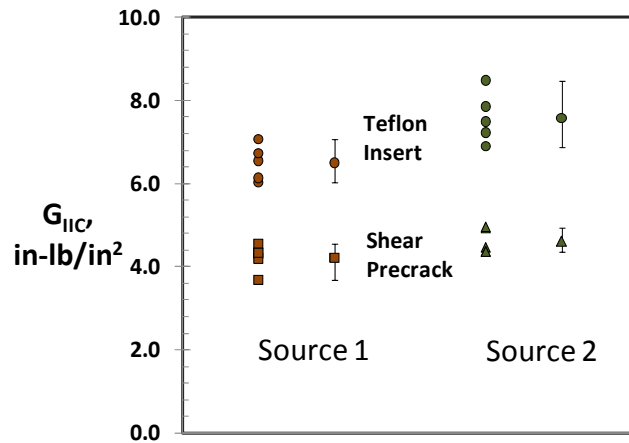


Fig.12 Fracture toughness values for both sources

	Specimen ID	PC G_{IIC} (in-lb/in ²)	NPC G_{IIC} (in-lb/in ²)
Source1	187	4.32	6.55
	186	3.69	7.06
	213	4.55	6.03
	206	4.20	6.14
	220	4.34	6.73
	Average	4.22	6.50
Source2	1S	4.92	8.48
	16TF	4.46	7.49
	09CF	4.36	7.22
	12CFHW	4.36	6.89
	12TFHW	4.95	7.85
	Average	4.61	7.58

Table 2. Non pre-crack and pre-crack mode II interlaminar fracture toughness.

The fatigue tests were run at loads corresponding to the different percentages of G_{IIC} as shown in table 3. The tabulated pre-crack mode II delamination onset data measurements for both sources are given in Appendix 1. Table 3 shows the $G_{II\max}$ values used to calculate P_{\max} for the fatigue tests. The actual $G_{II\max}$ values shown in figures 13 and 14, and tables A1-3, are adjusted by using the measured precrack lengths in equation 4.

Figure 13 shows the delamination onset data and curve fits for both manufacturers' specimens. The combined delamination onset threshold data from both suppliers are shown in figure 14 along with a fit to the data. The PC fracture toughness data appears on the left side of the plots. The data presented in Figure 13 demonstrated very consistent results from both manufacturers as shown in Figure 14.

Source 1		Source 2	
$G_{IICAVG} = 4.22$ in-lb/in ²		$G_{IICAVG} = 4.61$ in-lb/in ²	
50% G_{\max}	2.11	50% G_{\max}	2.31
40% G_{\max}	1.69	40% G_{\max}	1.84
30% G_{\max}	1.27	30% G_{\max}	1.38
20% G_{\max}	0.84	20% G_{\max}	0.92

Table 3. $G_{II\max}$ levels used to calculate P_{\max} for each fatigue specimen.

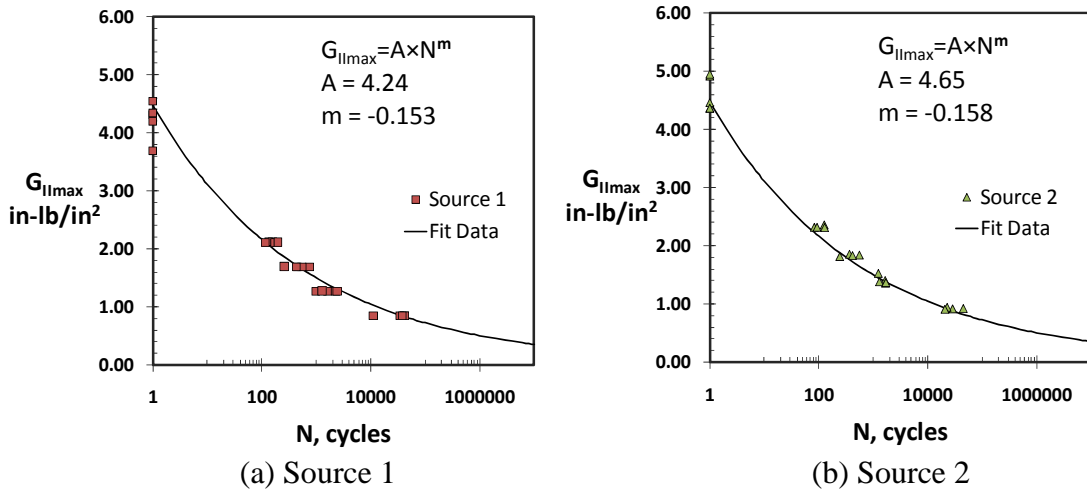


Fig.13 Power law fits applied to the delamination onset threshold data.

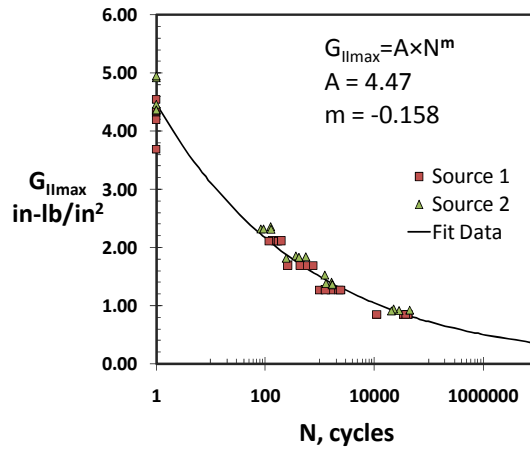
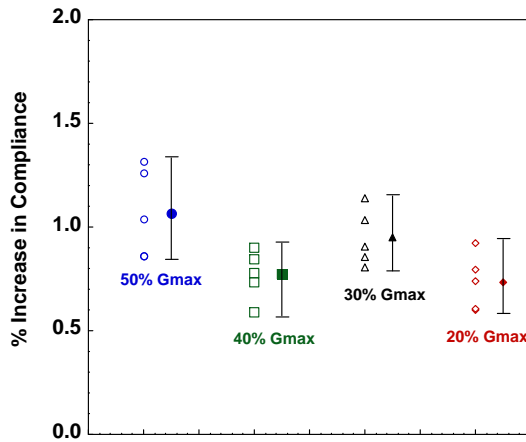
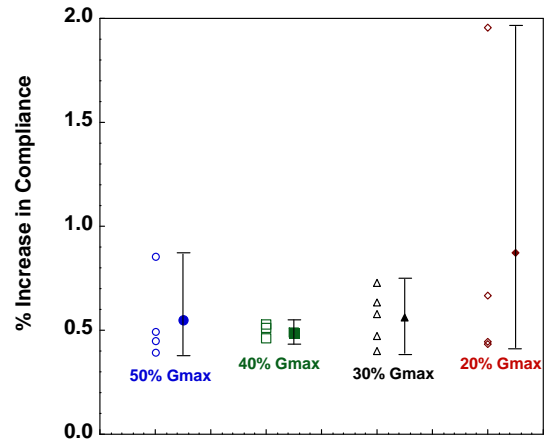


Fig.14 Power law fit applied to the delamination onset threshold data for all specimens.

The percent change in initial compliance at the onset of delamination growth was also calculated and plotted in Figure 15. The individual data points appear alongside an average value with corresponding error bars. The change in stiffness is similar to the one percent increase in compliance, which the Mode I fatigue standard prescribes as the onset value [6].



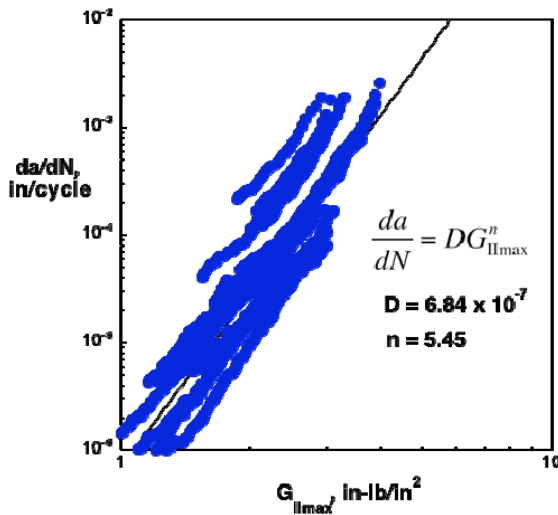
(a) Source 1



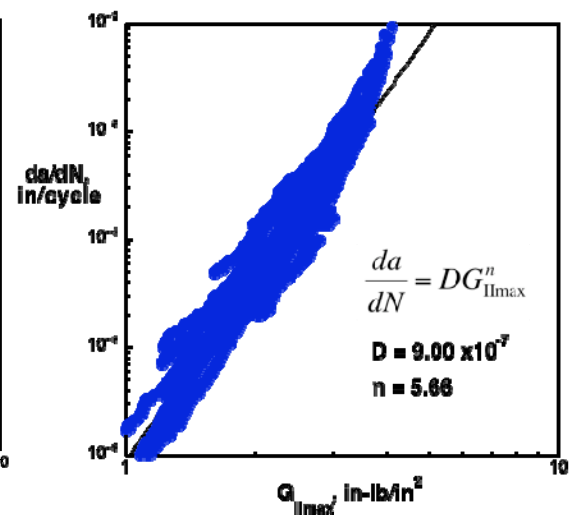
(b) Source 2

Fig.15 Percent increase in initial compliance at the onset of stable delamination growth.

The delamination crack growth results are summarized in Figure 16. Figure 16 shows the delamination growth laws derived by combining results for all five cyclic load levels into one log-log plot for the Source 1 (fig. 16a) and Source 2 (fig.16b) specimens.



(a) Source 1



(b) Source 2

Fig.16 Power law fits applied to the delamination growth data.

Discussion

The difference between the response of precracked and non-precracked specimens demonstrated the importance of using the proper data and testing method when using material data for delamination onset predictions. Both the interlaminar fracture toughness and the fatigue delamination onset are influenced greatly by the presence of a Teflon insert or a precrack. The importance of this difference is illustrated in figure 17, which compares the fatigue delamination onset behavior between precracked and non-precracked specimens [7]. The static fracture toughness values are shown along the y-axis of this linear-log plot, corresponding to $N = 1/4$ cycle. Not only is there a significant difference in the interlaminar fracture toughness values, but there are order of magnitude differences in fatigue delamination onset lives. The difference in cycles to onset becomes larger as the load decreases. Hence, the fatigue delamination onset behavior is strongly affected by the condition of the delamination front, and this information must be considered before using these data for analysis.

The fatigue delamination behavior of precracked and non-precracked fatigue specimens is shown schematically in Figure 18. For the precracked specimen tests, the initial instability in the delamination growth rate is denoted by a high growth rate that rapidly decays to a minimum after which stable increasing growth rates are observed. In contrast, for the test from a Teflon insert, the growth rate starts low and increases at a relatively constant G_{\max} level, until it reaches a point where the Paris law crack growth rate begins. This difference in behavior can be explained by considering how mode II shear delaminations initiate and propagate. Shear delaminations propagate through the coalescence of micro-tension cracks formed by the resolved shear stress ahead of the delamination crack front [8]. In addition to creating the precracked zone, the precracking process creates an area of uncoalesced microcracks ahead of the delamination front. The rapid initial growth of the PC specimens corresponds to the coalescence of these voids. When the formation of new voids and the coalescence of old voids have reached a steady state, the growth rate reaches a minimum. Conversely, cycling from the insert requires the initial formation of voids before the crack can grow, thus slowing the initial growth rate. When these voids begin to coalesce, stable growth begins.

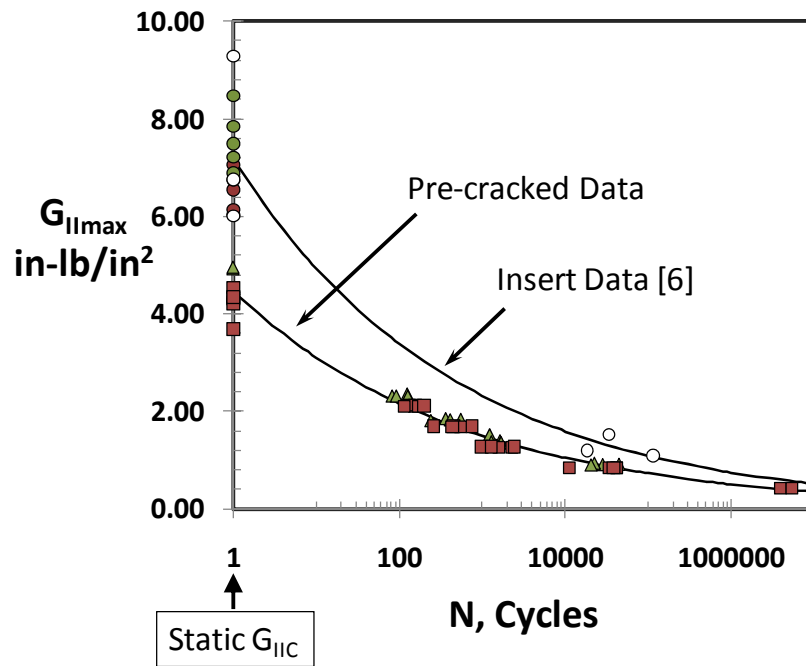


Fig.17 A comparison of fatigue onset behavior between precracked and nonprecracked specimens..

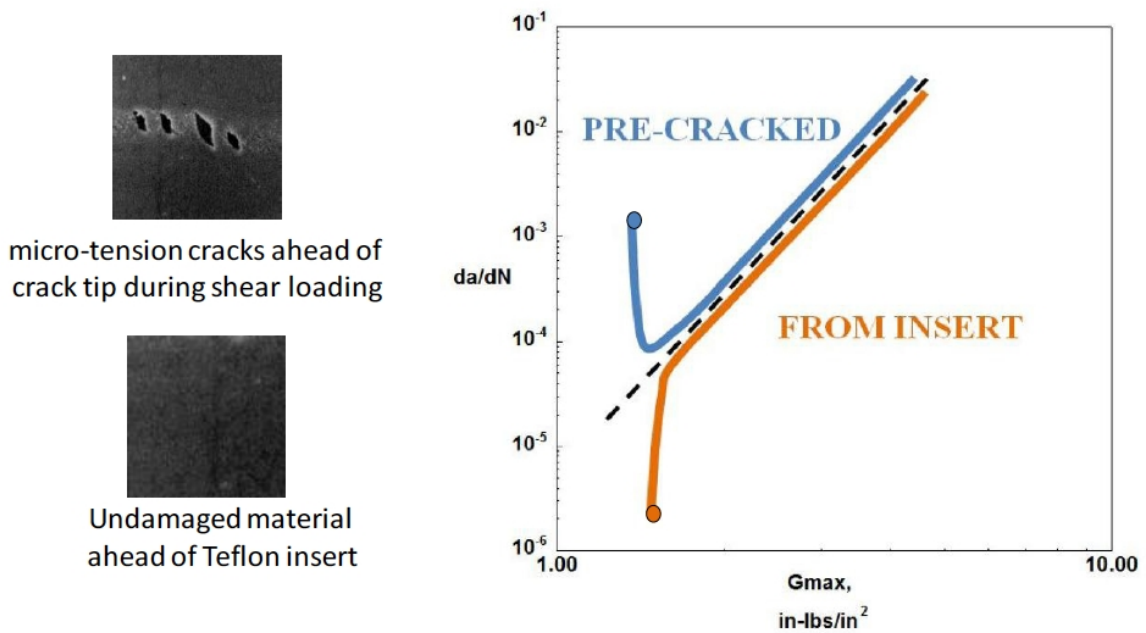


Fig.18 Fatigue onset behavior compared for precracked a non-precracked specimens.

Summary

Mode II interlaminar fracture toughness and delamination onset and growth characterization data were generated for IM7/8552 graphite epoxy composite materials from two suppliers for use in fracture mechanics analyses. The results for material produced by the two suppliers were similar for all material property values measured.

Insight was gained into testing that should be valuable for current and future material property standards. The draft ASTM procedure for G_{IIc} was followed and produced consistently repeatable interlaminar fracture toughness values. Furthermore, the testing procedures developed in this study, and the associated test results, will be useful for developing mode II fatigue standards. Methods were developed to parse and analyze fatigue data. Development of a Mode II fatigue delamination onset curve for precracked specimens and specimens with inserts were discussed. The effects of performing material property tests from either precracks or inserts was discussed and compared. Testing from a precracked specimen gave more conservative properties than testing from an insert, for both interlaminar fracture toughness and fatigue onset data.

References

- [1] ASTM Draft Standard Test Method for Determination of the Mode II Interlaminar Fracture Toughness of Unidirectional Fiber Reinforced Polymer Matrix Composites using the End-Notched Flexure (ENF) Test.
- [2] Fracture Technology Associates, Bethlehem, PA,
<http://www.fracturetech.com/index.html>.
- [3] D. Broek, *Elementary Engineering Fracture Mechanics*, 1991, p.124.
- [4] ASTM International, E 647-00, "Standard Test Method for Measurement of Fatigue Crack Growth Rates".
- [5] P. C. Paris, M. P. Gomez and W. E. Anderson, "A Rational Analytic Theory of Fatigue," *The Trend in Engineering* (1961). 13, pp. 9-14.
- [6] Standard Test Method for Mode I Fatigue Delamination Growth Onset of Unidirectional Fiber- Reinforced Polymer Matrix Composites, ASTM standard D6115-97, American Society for Testing and Materials Annual Book of standards, Vol. 15.03, 1997, pp. 338-343.
- [7] R. Martin, U.S. Army European Research Office Report - Report# N68171-98-M-5177, 1998.
- [8] O'Brien, T.K., "Composite Interlaminar Shear Fracture Toughness: G_{IIc} : Shear Measurement or Sheer Myth?", *Composite Materials: Fatigue and Fracture, Seventh Volume, ASTM STP 1330*, 1998, pp. 3-18.

APPENDIX 1 – Tabulated Data

This appendix tabulates the data used in this report for future reference. Specimen thicknesses and widths, measured at three locations along the length and averaged, are shown in Table A1 for both manufacturers (referred to as Source 1 and Source 2). The non-precracked and precracked compliance calibration coefficients are summarized in tables A2 and A3 below for Source 1 and Source 2 specimens, respectively. The fatigue onset data is summarized in table A4 for both sources

Source 1			Source 2		
Specimen ID	Width, B (in)	Thickness (in)	Specimen ID	Width, B (in)	Thickness (in)
181	0.992	0.1770	03CF	0.999	0.1723
182	0.991	0.1773	09CF	0.997	0.1760
183	0.991	0.1767	10CF	0.998	0.1752
185	0.989	0.1777	12CF	0.998	0.1687
186	0.993	0.1778	06CFHW	0.997	0.1793
187	0.991	0.1765	09CFHW	0.997	0.1775
199	0.991	0.1768	12CFHW	0.997	0.1748
201	0.992	0.1772	13CFHW	0.998	0.1755
202	0.991	0.1767	1S	0.994	0.1727
203	0.991	0.1765	2S	0.991	0.1753
206	0.990	0.1787	4S	0.993	0.1728
207	0.990	0.1793	01TF	0.998	0.1742
208	0.988	0.1792	03TF	0.998	0.1713
209	0.991	0.1783	15TF	0.997	0.1677
210	0.989	0.1782	16TF	0.997	0.1715
213	0.986	0.1823	20TF	0.998	0.1720
214	0.990	0.1788	25TF	0.998	0.1725
216	0.990	0.1783	29TF	0.998	0.1698
218	0.991	0.1783	02TFHW	0.990	0.1748
219	0.990	0.1792	10TFHW	0.990	0.1760
220	0.986	0.1807	12TFHW	0.989	0.1763
223	0.990	0.1828	15TFHW	0.990	0.1723
224	0.987	0.1813	17TFHW	0.990	0.1720
225	0.988	0.1803	21TFHW	0.990	0.1765
226	0.989	0.1788	25TFHW	0.992	0.1767

Table A1. ENF specimen dimensions.

$G_{II\max}$ Level	Specimen ID	Insert Configuration		Pre-Cracked Configuration	
		$m \times 10^{-5}$ (in ² -lb ⁻¹)	$A \times 10^{-5}$ (in/lb)	$m \times 10^{-5}$ (in ² -lb ⁻¹)	$A \times 10^{-5}$ (in/lb)
Static (100%)	187	2.6415	14.446	2.6843	14.564
	186	2.7341	14.394	2.6737	14.541
	213	2.4445	13.710	2.5445	13.636
	206	2.7227	14.463	3.0323	14.309
	220	2.5541	13.814	2.8471	13.836
50%	181	2.5861	14.721	2.5861	14.733
	199	2.5731	14.456	2.6077	14.380
	209	2.5086	14.694	2.7412	14.280
	214	2.4770	14.090	2.5395	13.990
	223	2.4366	13.843	2.3167	13.641
40%	182	2.5812	14.327	2.3375	14.604
	201	2.5652	14.457	2.6434	14.335
	207	2.5837	14.604	2.6963	14.145
	216	2.5558	14.294	2.5305	14.274
	224	2.4843	14.389	2.4869	14.004
30%	183	2.5122	14.232	2.4849	14.259
	202	2.5978	14.494	2.5067	14.369
	208	2.6412	14.595	2.5936	14.202
	218	2.5643	14.178	2.4898	14.015
	225	2.5974	14.476	2.5368	14.057
20%	185	2.4866	14.556	2.4325	14.424
	203	2.5760	14.604	2.5157	14.352
	210	2.5885	14.614	2.5925	14.263
	219	2.6300	13.888	2.5180	13.872
	226	2.5991	14.591	2.5596	14.246

Table A2. Source 1 compliance calibration curve coefficients.

$G_{II\max}$ Level	Specimen ID	Insert Configuration		Pre-Cracked Configuration	
		$m \times 10^{-5}$ (in ² -lb ⁻¹)	$A \times 10^{-5}$ (in/lb)	$m \times 10^{-5}$ (in ² -lb ⁻¹)	$A \times 10^{-5}$ (in/lb)
Static (100%)	1S	3.1556	13.625	3.3283	15.064
	16TF	2.5786	14.231	2.5454	15.316
	09CF	2.8193	15.033	3.1732	14.987
	12CFHW	2.5424	14.783	2.8841	14.902
	12TFHW	2.7839	14.313	3.0763	14.506
50%	2S	2.8559	15.413	2.9685	15.264
	3CF	2.8934	15.305	2.9167	15.703
	10CF	2.9075	15.126	2.9479	15.129
	10TFHW	2.8235	15.359	3.0579	14.928
	29TF	3.0559	16.469	3.1425	16.513
40%	4S	2.9464	15.233	2.8777	15.141
	13CFHW	2.8328	15.013	2.7837	14.864
	15TFHW	2.9856	15.644	2.9545	15.493
	20TF	3.0174	16.035	3.0360	15.771
	21TFHW	2.7465	14.837	2.7322	14.842
30%	01TF	2.8563	15.642	2.7739	15.458
	02TFHW	2.8688	15.154	2.8589	15.006
	09CFHW	2.8417	14.643	2.6388	14.758
	15TF	3.1789	16.662	3.1954	16.742
	17TFHW	3.0134	15.494	3.0389	15.209
20%	03TF	3.1408	16.167	3.4396	16.548
	06CFHW	2.7612	14.538	2.6826	14.446
	12CF	3.2024	16.954	3.2070	16.450
	25TF	2.9606	15.339	2.8069	15.263
	25TFHW	2.8229	14.864	2.7799	14.690

Table A3. Source 2 compliance calibration curve coefficients.

$G_{II\max}$ Level	Specimen ID	$G_{II\max}$ (in-lb/in ²)	Cycles to Onset
Source 1-50%	181	2.1133	156
	199	2.1197	133
	209	2.1039	170
	214	2.1079	116
	223	2.1174	199
Source 1-40%	182	1.6939	257
	201	1.6895	449
	207	1.6924	746
	216	1.6861	545
	224	1.6872	436
Source 1-30%	183	1.2681	1597
	202	1.2699	987
	208	1.2734	1275
	218	1.2696	2246
	225	1.2718	2420
Source 1-20%	185	0.8445	41642
	203	0.8446	11080
	210	0.8482	34114
	219	0.8487	41643
	226	0.8490	38271
Source 2-50%	3CF	2.3190	83
	10CF	2.3592	126
	10TFHW	2.3146	128
	29TF	2.3188	93
Source 2-40%	4S	1.8559	366
	13CFHW	1.8414	557
	15TFHW	1.8328	416
	20TF	1.8161	243
Source 2-30%	01TF	1.5271	1242
	02TFHW	1.4049	1654
	09CFHW	1.3827	1302
	15TF	1.3589	1678
	17TFHW	1.3681	1706
Source 2-20%	06CFHW	0.91766	28653
	12CF	0.94497	22733
	25TF	0.92442	44969
	25TFHW	0.91098	20725

Table A4. Pre-crack mode II cycles to delamination onset.

APPENDIX 2 –Delamination Growth Data

Delamination growth data are shown along with fits for each load level in figures A1 and A2 below for Source 1 and Source 2 specimens, respectively.

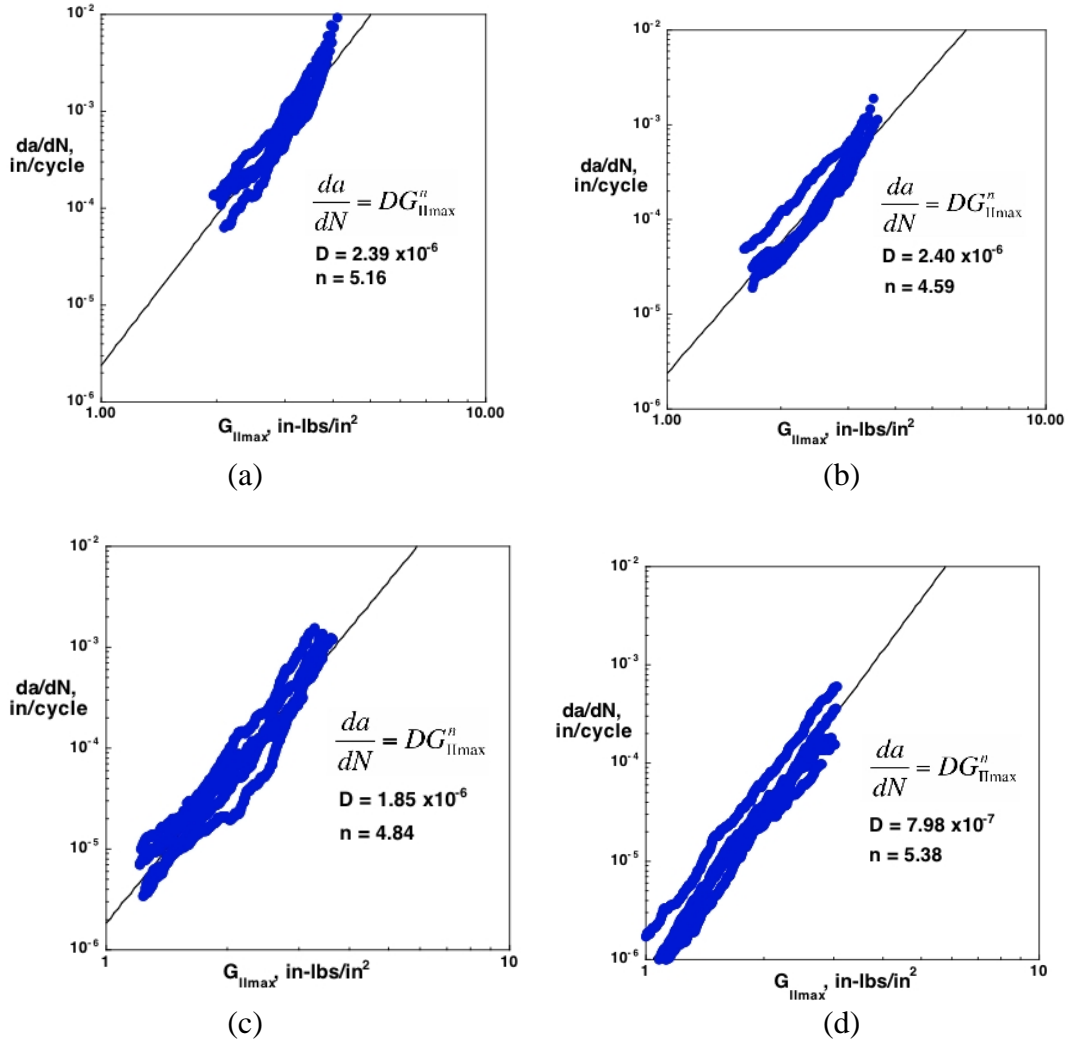


Fig.A1. Experimental data and power law fits applied to the delamination growth data from Source 1 for the 50% (a), 40%(b), 30%(c) and 20%(d) load level tests.

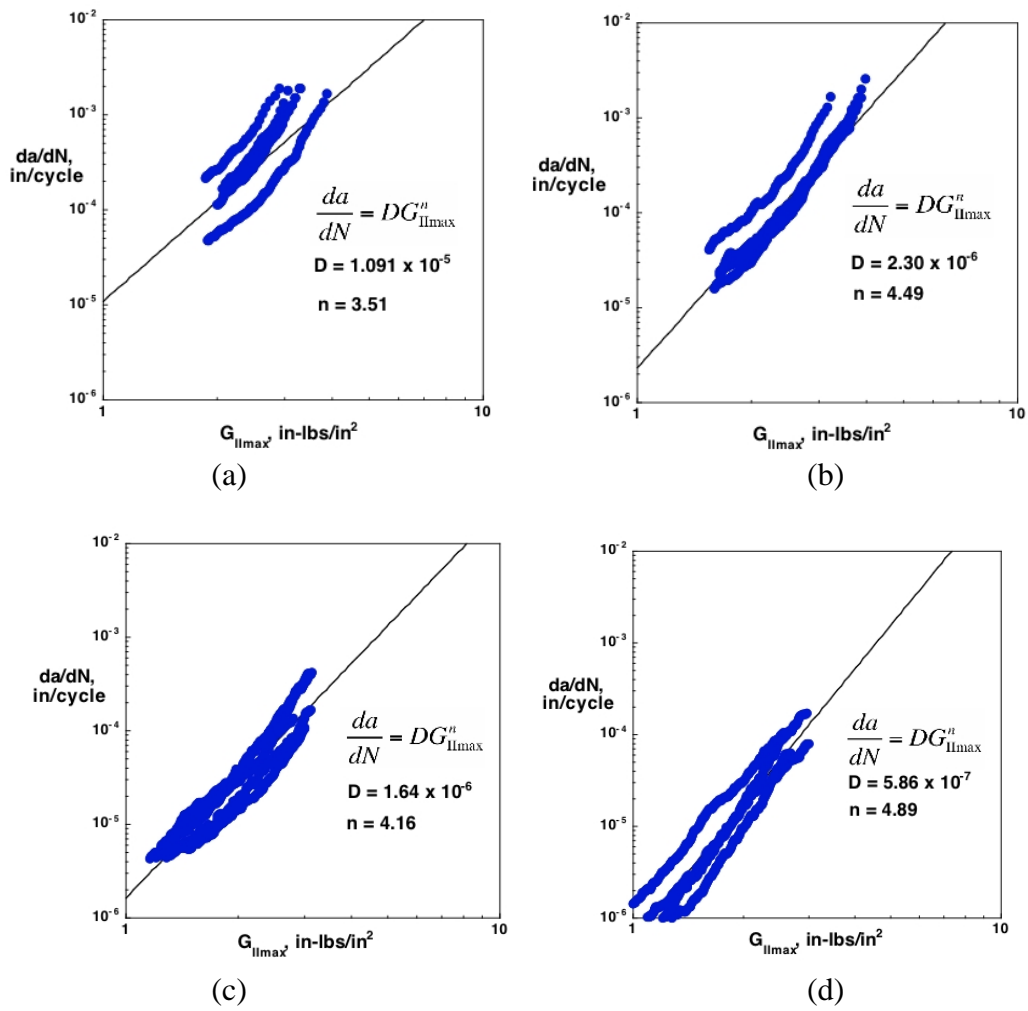


Fig.A2. Experimental data and power law fits applied to the delamination growth data from Source 2 for the 50% (a), 40%(b), 30%(c) and 20%(d) load level tests.

REPORT DOCUMENTATION PAGE

*Form Approved
OMB No. 0704-0188*

The public reporting burden for this collection of information is estimated to average 1 hour per response, including the time for reviewing instructions, searching existing data sources, gathering and maintaining the data needed, and completing and reviewing the collection of information. Send comments regarding this burden estimate or any other aspect of this collection of information, including suggestions for reducing this burden, to Department of Defense, Washington Headquarters Services, Directorate for Information Operations and Reports (0704-0188), 1215 Jefferson Davis Highway, Suite 1204, Arlington, VA 22202-4302. Respondents should be aware that notwithstanding any other provision of law, no person shall be subject to any penalty for failing to comply with a collection of information if it does not display a currently valid OMB control number.
PLEASE DO NOT RETURN YOUR FORM TO THE ABOVE ADDRESS.

1. REPORT DATE (DD-MM-YYYY) 01-08-2010		2. REPORT TYPE Technical Memorandum		3. DATES COVERED (From - To)	
4. TITLE AND SUBTITLE Mode II Interlaminar Fracture Toughness and Fatigue Characterization of a Graphite Epoxy Composite Material				5a. CONTRACT NUMBER	
				5b. GRANT NUMBER	
				5c. PROGRAM ELEMENT NUMBER	
6. AUTHOR(S) O'Brien, T. Kevin; Johnston, William M.; Toland, Gregory J.				5d. PROJECT NUMBER	
				5e. TASK NUMBER	
				5f. WORK UNIT NUMBER 698259.02.07.07.03.03	
7. PERFORMING ORGANIZATION NAME(S) AND ADDRESS(ES) NASA Langley Research Center Hampton, VA 23681-2199				8. PERFORMING ORGANIZATION REPORT NUMBER L-19898	
9. SPONSORING/MONITORING AGENCY NAME(S) AND ADDRESS(ES) National Aeronautics and Space Administration Washington, DC 20546-0001				10. SPONSOR/MONITOR'S ACRONYM(S) NASA	
				11. SPONSOR/MONITOR'S REPORT NUMBER(S) NASA/TM-2010-216838	
12. DISTRIBUTION/AVAILABILITY STATEMENT Unclassified - Unlimited Subject Category 24 Availability: NASA CASI (443) 757-5802					
13. SUPPLEMENTARY NOTES					
14. ABSTRACT Mode II interlaminar fracture toughness and delamination onset and growth characterization data were generated for IM7/8552 graphite epoxy composite materials from two suppliers for use in fracture mechanics analyses. Both the fracture toughness testing and the fatigue testing were conducted using the End-notched Flexure (ENF) test. The ENF test for mode II fracture toughness is currently under review by ASTM as a potential standard test method. This current draft ASTM protocol was used as a guide to conduct the tests on the IM7/8552 material. This report summarizes the test approach, methods, procedures and results of this characterization effort.					
15. SUBJECT TERMS Graphite-epoxy composites; Fracture mechanics; Fatigue; Delamination					
16. SECURITY CLASSIFICATION OF:			17. LIMITATION OF ABSTRACT	18. NUMBER OF PAGES	19a. NAME OF RESPONSIBLE PERSON
a. REPORT	b. ABSTRACT	c. THIS PAGE			STI Help Desk (email: help@sti.nasa.gov)
U	U	U	UU	32	19b. TELEPHONE NUMBER (Include area code) (443) 757-5802